RESEARCH ARTICLE

Synthesis, Docking Study and Antitumor Activity of New Pyrido[1,2-a] Pyrimidine Schiff Base Derivatives as Non-classical Antifolate

Rafid M. Hashim[1*], Monther F Mahdi[2], Inam S. Arif[3]

[1]*College of Pharmacy, Department of Pharmaceutical Chemistry, Uruk University, Baghdad, Iraq*
[2]*College of Pharmacy, Department of Pharmaceutical Chemistry, Mustansiriyah University, Baghdad, Iraq*
[3]*College of Pharmacy, Department of Pharmacology & Toxicology, Mustansiriyah University, Baghdad, Iraq*

Received: 20th September, 2021; Revised: 22nd October, 2021; Accepted: 15th November, 2021; Available Online: 25th December, 2021

ABSTRACT

Pyrido[1,2 a]pyrimidine Schiff base derivatives not reported previously were synthesized, and their chemical structures were confirmed by physicochemical and spectral characterization. The synthesized entities were evaluated for their antitumor activity against (MCF-7) cells by the 3-(4,5-dimethylthiazol-2-yl)-2,5-diphenyltetrazolium bromide (MTT) method, with methotrexate (MTX) positive control. Compounds 1 and 5 show the highest results.

In silico docking study was performed using gold software to evaluate the inhibitory effect of synthesized entities on human Dihydrofolate reductase and Thymidylate Synthase enzyme. Furthermore, these compounds were also tested for their cytotoxicity against MCF-10 cells confirming their non-toxic behavior against normal cells and selectivity towards cancerous one. The pharmacokinetic parameters were also evaluated *In silico*, indicating an excellent oral bioavailability.

Keywords: Dihydrofolate reductase (DHFR), MTX, Pyrido[1,2 a]pyrimidine, Schiff base, Thymidylate synthase (TS).

International Journal of Drug Delivery Technology (2021); DOI: 10.25258/ijddt.11.4.26

How to cite this article: Hashim RM, Mahdi MF, Arif IS. Synthesis, Docking Study and Antitumor Activity of New Pyrido[1,2-a] Pyrimidine Schiff Base Derivatives as Non-classical Antifolate. International Journal of Drug Delivery Technology. 2021;11(4):1275-1281.

Source of support: Nil.

Conflict of interest: None

INTRODUCTION

The study of novel chemical entities for cancer treatment is a new field of study in pharmaceutical research. Today, cancer is a disease that is having a significant impact on human health across the world.

Toxicity is an increasing concern with modern cancer therapies, and extreme adverse effects accompany contemporary anticancer medicines. For these reasons, more effective, selective, and safe chemotherapeutic drugs are required to treat malignancies.[1]

In this context, enzymes with essential roles like DHFR and TS are exciting targets for drug chemotherapy. The inhibition of these enzymes leads to interrupting DNA production and stop cell division.[2]

The primary rationale for creating medicines based on tiny organic compounds such as nucleoside analogs is the high compatibility between small chemical entities and biological systems.[3] Fluorouracil, gemcitabine, capecitabine, and floxuridine are several pyrimidine antagonists utilized in cancer treatments.[4] In this respect, because of its structural similarities with nucleobases pyridopyrimidines are a vital class of aza-bridgehead fusing heterocyclic compounds and their robust biology.[5] Fused pyrimidines have been discovered to have antiviral,[6] antibacterial,[7] anti-HIV.[8] They are extensively used to treat neurodegenerative disorders like Parkinson's disease,[9] anti-anxiety disorders,[10] and depression.[11] Their applications are especially attractive due to the inhibition of multidrug resistance.[12] Fused pyrimidine antifolates act as antitumor agents, thus making folate metabolism an attractive target for cancer chemotherapy.[13]

These lipophilic chemicals can enter the cell through passive diffusion, with non-classical antifolates distinguished by the Suppression of the glutamic chain of the folic acids scepter (2). These compounds are not substrates for the active transportation mechanisms for folates. They have the benefit of being active in methotrexate-resistant cancer cells due to transport abnormalities.[14]

Schiff Basis also constitutes an essential chemical class in which numerous applications in analysis, biology, and inorganic chemistry are widely exploited.[15]

Due to the broad spectrum of biological activities such as antibacterial, anti-inflammatory, anticancer, etc., the Schiff base became significant in medical and pharmaceutical areas. Azomethine's nitrogen atom may establish an H-bond with an active cell component and interfere with ordinary cell activities.[16]

**Author for Correspondence: rafid1983@gmail.com*

MATERIALS AND METHODS

Chemistry

Chemicals were purchased from (Sigma-Aldrich, Germany, HI-Media, India, and GK Bio-Technology, China); all other solvents and chemicals were of AnalaR grade and generally used as obtained from commercial suppliers.

The melting point was measured by using the open capillary method with electrical melting point apparatus. The IR bands were recorded using Shimadzu (Japan), one-dimensional Hydrogen-1 Nuclear Magnetic Resonance (^{1}HNMR) spectra were recorded using Bruker (AVANCE) 400 MHz NMR instrument.

The chemical synthesis of target compounds was achieved following the procedure shown in scheme 1.

Compound I: Synthesis of 2H pyrido [1, 2-a] pyrimidine-2,4(3H)dione

2-aminopyridine (10 gm, 0.106 moles) and diethyl malonate (21.22 gm, 0.132 moles) were mixed and heated under gentle reflux in a flask fitted with a still head until the theoretical quantity of ethyl alcohol was collected. The mixture was then chilled and filtered, and the product was washed with methanol and dried. This compound was recrystallized from water.[17]

The percentage yield is 85%, M.P. 277°C (decomposed), FT-IR band absorption characteristic(ν, cm-1): 2640-2810 (broad enolic OH), 1632 (C=O amide), 1595 (C=N of imine). The ^{1}H-NMR spectra (500 MHz, DMSO) δ: 3.2 (2H,s, methine), 6.5 (1H, t, aromatic), 7.1 (1H, t, aromatic), 7.4 (1H, t, aromatic), 8.1 (1H, t, aromatic).

Compound II: Synthesis of 3-formyl-2H-pyrido[1,2a] pyrimidine-2,4-(3H) dione

Phosphoryl chloride (3 mL) is gently added to N, N-dimethyl-formamide (30 mL) while chilling in an ice bath. The mixture is next heated on the water bath for 20 minutes with 2H-pyrido[1,2-a]pyrimidine-2,4(3H) dione (4.85 gm, 1 mol). After cooling to room temperature, the mixture containing the intermediate 3-dimethylamino methylene-3H-pyrido[1,2-a] pyrimidine-2,4(3H) dione is gently poured into 50 mL 5N sodium hydroxide with vigorous stirring. When the process becomes exothermic, ice is added. After that, the mixture is acidified with dilute hydrochloric acid. A transparent solution is produced, followed by solid precipitation collected and dried using a filter funnel. Recrystallization from N, N-dimethylformamide.[18] The percentage yield is 85%, MP 277°C (decomposed), fourier transform infrared spectroscopy (FTIR) band absorption characteristic (ν, cm^{-1}): 2773 (C-H aldehyde), 1732 (C=O aldehyde), 1654 (C=O pyridopyrimidine ring). The ^{1}HNMR spectra (500 MHz, DMSO) δ: 4.03 (1H, d, methine), 6.32 (1H, d, aromatic), 6.4 (1H, d, aromatic), 6.93 (1H, d, aromatic), 7.42 (1H, d, aromatic), 10.10 (1H, d, aldehyde).

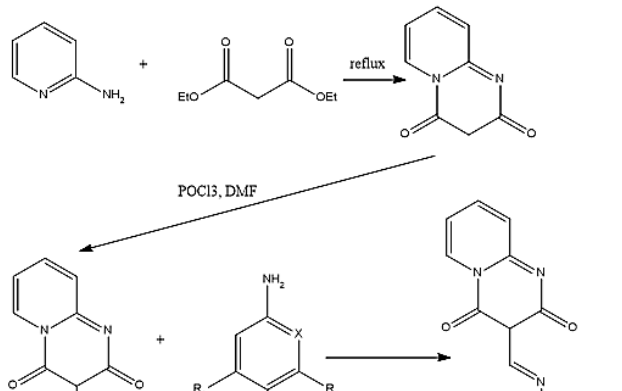

Comp.	X	R1	R2	R3
M1	C	OCH3	OCH3	OCH3
M2	N	CF3	H	H
M3	N	H	H	CF3
M4	N	H	CF3	H
M5	N	NH2	F	F

Scheme 1: Synthesis of final compounds

General Chemical Synthesis of Schiff Bases

A combination of equimolar amounts (5 mmol) of the II and the amino compound (5 mmol) in absolute dry methanol (30 mL) containing a catalytic quantity (2 drops) of glacial acetic acid was refluxed for 4 hours. A solid produced product was filtered, rinsed and dried with hot water.[19]

Compound M1: synthesis of 3-(((3,4,5-trimethoxyphenyl) imino)methyl)-2H-pyrido[1,2-a]pyrimidine-2,4(3H)-dione

In absolute dry methanol (30 mL) containing a catalytic quantity of glacial acetic acid (2 drops), an equimolar amount (0.95 g, 5 mmol) of the (II) and the 3,4,5-tri-methoxy aniline (0.91 g, 5 mmol) was reacted under reflux for 4 hours. Filtration was used to separate the solid product, which was then washed with hot water and dried. The percentage yield is 82%, MP 225°C, FT-IR band absorption characteristic(ν, cm^{-1}): 1708 (C=O of pyridopyrimidine ring), 1647 (C=N of imine), 1018 (C-O of methoxy), The 1HNMR spectra (500 MHz, DMSO) δ: 3.73 (3H, s, methoxy), 3.82 (1H, d, methine), 3.93 (6H, s, methoxy), 6.2 (1H, d, aromatic), 7.11 (1H, d, aromatic), 7.22 (1H, d, aromatic), 7.45-7.36 (1H, m, aromatic), 7.51 (1H, d, aromatic), 8.58 (1H, d, imine).

Compound M2: Synthesis of 3-(((6-(trifluoromethyl) pyridin-2-yl)imino)methyl)-2H-pyrido[1,2-a]pyrimidine-2,4(3H)-dione:

In absolute dry methanol (30 mL) containing a catalytic quantity of glacial acetic acid (2 drops), an equimolar amount (0.95 g, 5 mmol) of the (II) and the 6-(trifluoromethyl)pyridine-2-amine (0.81 g, 5 mmol) of the (II) and the 6-(trifluoromethyl) pyridine-2-amine (0.81 g, 5 mmol) of the Filtration was used to separate the solid product, which was then washed with hot water and dried. The percentage yield is 80%, MP 241°C, FT-IR band absorption characteristic(ν, cm^{-1}): 1705 (C=O of pyridopyrimidine ring), 1604 (C=N of imine), 1087 (C-F of trifluoromethyl), The ^{1}H-NMR spectra (500 MHz, DMSO) δ: 2.75 (1H, d, methine), 6.34 (1H, d, aromatic), 7.25 (1H, d, aromatic), 7.41-7.49 (1H, m, aromatic), 7.67 (1H, d, aromatic), 7.76 (1H, d, aromatic), 7.96 (1H, d, aromatic), 8.23 (1H, d, aromatic), 8.96 (1H, d, imine).

Compound M3: Synthesis of 3-(((4-(trifluoromethyl) pyridin-2-yl)imino)methyl)-2H-pyrido[1,2-a]pyrimidine-2,4(3H)-dione:

In absolute dry methanol (30 mL) containing a catalytic quantity of glacial acetic acid (2 drops), an equimolar amount (0.95 g, 5 mmol) of the (II) and the 4-(trifluoromethyl)pyridine-2-amine (0.81 g, 5 mmol) of the (II) and the 4-(trifluoromethyl) pyridine-2-amine (0.81 g, 5 mmol) of the Filtration was used to separate the solid product, which was then washed with hot water and dried. The percentage yield is 80%, M.P. 241°C, FT-IR band absorption characteristic(ν, cm^{-1}): 1711 (C=O of pyridopyrimidine ring), 1622 (C=N of imine), 1072 (C-F of trifluoromethyl), The ^{1}HNMR spectra (500 MHz, DMSO) δ: 2.83 (1H, d, methine), 6.37 (1H, d, aromatic), 7.20 (1H, d, aromatic), 7.44-7.53 (1H, m, aromatic), 7.71 (1H, d, aromatic), 7.79 (1H, d, aromatic), 7.92 (1H, d, aromatic), 8.33 (1H, d, aromatic), 8.91 (1H, d, imine).

Compound M4: Synthesis of 3-(((5-(trifluoromethyl) pyridin-2-yl)imino)methyl)-2H-pyrido[1,2-a]pyrimidine-2,4(3H)-dione:

Under reflux for 4 hours, an equimolar quantity (0.95 g, 5 mmol) of the (II) and the 5-(trifluoromethyl)pyridine-2-amine (0.81 g, 5 mmol) in absolute dry methanol (30 mL) containing a catalytic amount of glacial acetic acid (2 drops) was reacted. Filtration was used to separate the solid product, which was then washed with hot water and dried. The percentage yield is 82%, MP 225°C, FT-IR band absorption characteristic(ν, cm^{-1}): 1708 (C=O of pyridopyrimidine ring), 1647 (C=N of imine), 1018 (C-O of methoxy). The ^{1}HNMR spectra (500 MHz, DMSO) δ: 2.81 (1H, d, methine), 6.33 (1H, d, aromatic), 7.45-7.34 (1H, m, aromatic), 7.85 (1H, m, aromatic), 8.03 (1H, d, aromatic), 8.25 (1H, d, aromatic), 8.6 (1H, d, aromatic), 8.96 (1H, d, imine), 10.04 (1H, d, aromatic).

Compound M5: synthesis of 3-(((6-amino-3,5-difluoropyridin-2-yl)imino)methyl)-2H-pyrido[1,2-a] pyrimidine-2,4(3H)-dione:

Under reflux for 4 hours, an equimolar quantity (0.95 g, 5 mmol) of the (II) and the 3,5-difluoropyridine-2,6-diamine (0.72 g, 5 mmol) were reacted in absolute dry methanol (30 mL) containing a catalytic amount of glacial acetic acid (2 drops). Filtration was used to separate the solid product, which was then washed with hot water and dried. The percentage yield is 82%, MP 225°C, FT-IR band absorption characteristic (ν, cm^{-1}): 1708 (C=O of pyridopyrimidine ring), 1647 (C=N of imine), 1018 (C-O of methoxy). The ^{1}HNMR spectra (500 MHz, DMSO) δ: 2.82 (1H, d, methine), 6.15 (2H, s, amino group), 6.93 (1H, d, aromatic), 7.45-7.35 (1H, m, aromatic), 7.74 (1H, m, aromatic), 7.96 (1H, d, aromatic), 8.25 (1H, d, aromatic), 8.96 (1H, d, imine).

Antitumor Activity

Cell Lines

In this investigation, the following cell lines were used:

- Breast cancer (MCF-7)
- Non-tumorigenic epithelial cell (MCF-10A)

Cell Maintenance

The cells were cultured in Dulbecco's Modified Eagle Medium (DMEM) medium supplemented with 10% fetal bovine serum (FBS), 1% L-Glutamine, and 1% Penicillin Streptomycin-Amphotericin B 100X antiseptic. Cells were grown in 75 cm^2 flasks and incubated at 37ºC in a combination of 5% CO_2 and 95% humidified air.[20] Once cell-containing flasks have attained 90% confluence, they have been passed under sterile conditions. They were washed with 5 mL of PBS and then incubated in the trypsin solution at 37°C for 2 minutes to remove the base of the flask. A 50 mL conical tube with an equivalent volume of full growth media was put in the cell suspension. At 1200 to 120 minutes, the cells were then centrifuged. After the supernatant was removed, the cell pellet was rearranged in a freshly enriched growth medium. Then, the cells were counted on a microscope hemocytometer and used accordingly.[21]

Cell Line Storage and Resuscitation

After a 75 cm^2 conflict, the cell suspension had been centrifuged 3 minutes at 1200 rpm. The cell pellet was then reconstituted in a 4 mL freezing medium and divided into 1 mL aliquots for cryovials. The cells were kept at –80°C for 24 hours before being placed in liquid nitrogen for long-term preservation. Cells frozen using liquid nitrogen were quickly coated at 37°C, then combined with a fresh 10 mL growing media. Before being placed in a 75 cm^2 flask and allowed to grow the cells were centrifugated and rebuilt in 25 mL fresh medium.[22]

MTT Assay for Cell Viability

The final compounds have been evaluated using the MTT test for malignant and non-cancerous cell effects. Total 100 liters of all suspension cells (MCF-7s) were dispersed on the 5×10^3 cells per well on a 96-well flat-bottom cultivation plate under normal circumstances for 24 hours; 4×10^3 cells per well for 48 hours and 3×10^3 cells per well for 72 hours. After 24 hours, the cells were treated with (1.52, 3.125, 6.25, 12.5, 25, 50, and 100 M). After 24, 48, and 72 hours of restoration time, the cell culture medium was removed. Cultivation was carried out in medium-growth crops for four hours at 37ºC with 30 µL MTT (3 mg/mL MTT in PBS) (3-(4,5- Dimethylthiazol-2-yl). This medium is gently reversed and taped to paper after 4 hours. In the control wells, just 100 l of growth media were utilized. Each well was given 100 l of dimethyl sulfoxide (DMSO), kept at ambient temperature and dark for around 15–20 minutes. A multiscan reader was used to measure each well's absorbance at 540 nm, with a wavelength of 650 nm utilized to correct for background absorbance.[23]

Determination of the Half Maximal Inhibitory Concentration (IC50)

The drug's IC50 may be determined by generating a dose-response curve and examining the impact of different antagonist dosages on reversing agonist activity. Calculating the dosage necessary to inhibit half of the agonist's maximum biological response yields IC50 values.[24]. The conditions

under which IC50 values are produced are essential. In general, the lower the agonist activity, the higher the inhibitor concentration. As the agonist concentration increases, so does the IC50 value.[25]

The IC50 shows the concentration of the tested chemicals (M1-17) necessary for 50% suppression of cell viability in an in vitro MTT experiment. The concentration range (M1-17) was 1.52–100 M, which was used to calculate the IC50 values.

Table 1: Chemical formula and structure of final compounds

Compound	*Chemical formula*	*Structure*
M1	$C_{18}H_{17}N_3O_5$	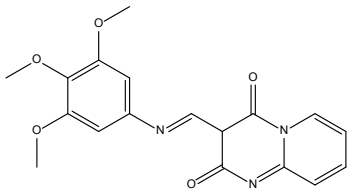
M2	$C_{15}H_9F_3N_4O_2$	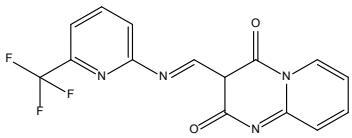
M3	$C_{15}H_9F_3N_4O_2$	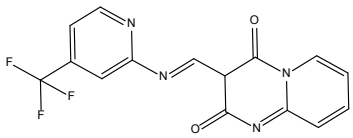
M4	$C_{15}H_9F_3N_4O_2$	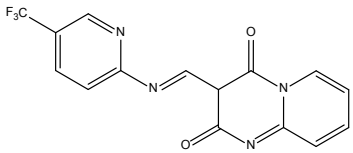
M5	$C_{14}H_9F_2N_5O_2$	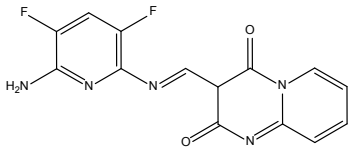

Data Analysis

All statistical analyses of MTT assay and IC50 data (M1-17) on cell lines were performed using the nonlinear curve fitting software (graph pad prism). One-way ANOVA evaluated a comparison between all groups within the same plate of MTT with Tukey test included in (GraphPad prism).[26] Statistical significance was defined as a value of (p) equal to 0.05.

RESULTS AND DISCUSSION

The compounds (M1-5) were successively synthesized and characterized. These compounds are listed in Table 1.

The Biological Effect of the Synthesized Compounds on the Cancerous and Normal Cell Lines

Effect on MCF-7 Breast Cancer Cell-line

IC_{50} values for Human Breast Cancer (MCF-7) and non-cancerous (MCF-10A) Cell Line summarized in Table 2.

Docking Study

The GOLD (Genetic Optimization for Ligand Docking) method is a genetic algorithm that docks flexible ligands into protein binding sites.[27] GOLD Suite has demonstrated flawless accuracy in posture prediction and outstanding outcomes in virtual screening.[28]

Docking was performed successfully for the final synthesized compounds $M_{(1-5)}$, using GOLD Suite software; the docking data were used to determine the selectivity and binding energies of the ligands for the protein (DHFR: PDB code: 3EIG) through studying the contact interactions among the active binding sites of the protein and designed compounds. The DHFR inhibitory activity of compounds $M_{(1-5)}$ and MTX were ranked based on their PLP fitness. The PLP fitness of the docked compounds on DHFR was found in the range of 69.68 to 85.61 as shown in Table 3.

ADMET Studies

The ADMET properties results of our synthesized analogs were studied by the input of a simplified molecular line-entry system of all derivatives that was generated with the

Table 2: Cytotoxicity of the final compounds and MTX as the standard against MCF-7 cell line

	IC50					
Cell line	*MTX*	*M1*	*M2*	*M3*	*M4*	*M5*
MCF-7	20.1	30.3	<100	<100	67.8	24.6
MCF-10A	<100	<100	<100	<100	<100	<100

Table 3: The binding energies for $M_{(1-5)}$ and MTX docked with DHFR enzyme (3EIG)

Comp.	*DHFR binding energy (PLP fitness)*	*# of H-bond*	*Amino acids included in H- bonding*
M1	71.95	4	SER59(2)*, Val115, Arg31
M2	70.87	3	Gly20, Ser59(3)*
M3	70.1	4	Gly20, Ser59(3)*
M4	70.82	2	Ala9, Thr56
M5	69.68	5	Gly20, Ser59(4)*
MTX	71.14	6	ASN64(2)*, Ala9, Thr56, Tyr121, Glu35

*number in brackets refers to the number of bonds with the same amino acid.

help of an online tool, that is, Swiss absorption, distribution, metabolism and excretion (ADME) server, to predict which of the synthesized ligands are susceptible to be given orally and to reveal the unharmed and potential drug candidate(s), to exclude the compounds that may fail in the following stages of the drug development because of the uncomplimentary ADME properties.[29]

We assessed all synthesized compounds for their pharmacokinetics and drug-likeness properties; some are listed in the table below.

DISCUSSIONS

The novel Pyrido[1,2-a]pyrimidine derivatives have progressively been synthesized, as validated by physical and spectroscopic data. The IR spectrum of the starting compound II shows a characteristic peak of aldehyde (2780 cm^{-1}, C-H and 1720, C=O) which was absent in the new derivatives M_{1-5} as it converted to imine (C=N), which appear at 1620 cm^{-1}.

In addition to these changes, the appearance of new peaks for aromatic substitution in the phenyl ring is significant, like (C-O) for methoxy in M1 and (C-F) in M2, M3, and M4 also (N-H) in M5.

The proton NMR displays the disappearance of aldehydic hydrogen at (10.10) ppm and the appearance of imine hydrogen at 8.58 ppm, which confirms the formation of the imine bond.

As concerning antitumor activity, Table 2 summarizes the results as it shows the activity of the synthesized compounds on both cancerous and non-cancerous cell line where for MCF-7 cell line, M5 and M1 show a good activity but still IC50 higher than that of MTX while M4 shows moderate activity.

Reasonably to estimate the selectivity of the final compounds towards the cancerous cell line, their effect against the non-cancerous cell line has to be estimated through (MCF-10A) cell line; this reveals that all compounds M_{1-5} show low toxicity, which gives a good sign about the selectivity of these compounds.

The Insilico pharmacokinetic study of the synthesized compounds summarized in Table 3 shows that all compounds have a TPSA value (76.68–102.7). The topological polar surface area (TPSA) is a crucial parameter that is closely related to bioavailability. As a result, the synthesized compound is predicted to have good GI absorption, while only M_2, M_3, and M_4 can cross BBB.

All compounds also satisfied Lipinski's criterion, which shows the characteristics of the medication and that the systemic circulation may be entered by all compounds (M_{1-5}). The cytotoxicity study does not contain a toxicity notice. The crystal structure of DHFR was gained from the protein data bank (PDB id: 3EIG), a MTX resistant mutant of human dihydrofolate reductase. The newly synthesized compounds were docked into the active site of the enzyme. The binding interaction and the amino acids involved are listed in Table 4.

Docking shows that compound M1 has the best fitting with the active site and the best gold score as compared with MTX. The docking of the synthesized compounds is shown in the Figures 1 to 6.

CONCLUSION

New compounds derived from Pyrido[1,2-a]pyrimidine containing Schiff base moiety were successfully synthesized and characterized. Among these compounds, M1 and M5 show a good antitumor activity with low cytotoxicity compared with MTX, and molecular docking study predicted that M1 has the best fitness with the active site of DHFR finding is compatible

Table 4: Some pharmacokinetic and drug-likeness properties for synthesized compounds M_{1-5}

Molecule	*TPSA*	*Ali Class*	*GI absorption*	*BBB permeant*	*Pgp substrate*	*Lipinski #violations*	*Bioavailability score*	*PAINS #alerts*
M1	91.48	Soluble	High	No	No	0	0.55	0
M2	76.68	Soluble	High	Yes	No	0	0.55	0
M3	76.68	Soluble	High	Yes	No	0	0.55	0
M4	76.68	Soluble	High	Yes	No	0	0.55	0
M5	102.7	Soluble	High	No	No	0	0.55	0

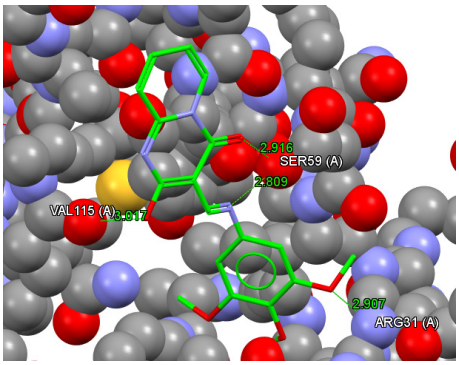

Figure 1: H-bond interaction for M1 binding with DHFR enzyme

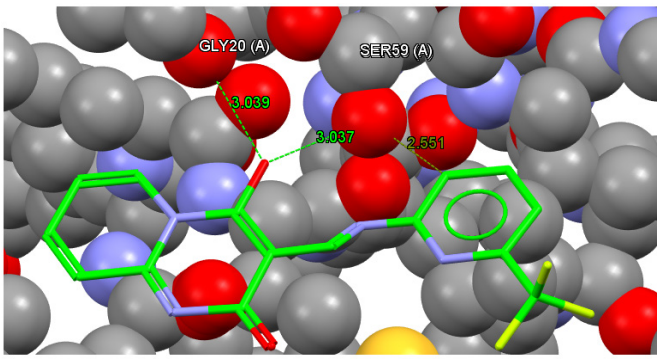

Figure 2: H-bond interaction for M2 binding with DHFR enzyme

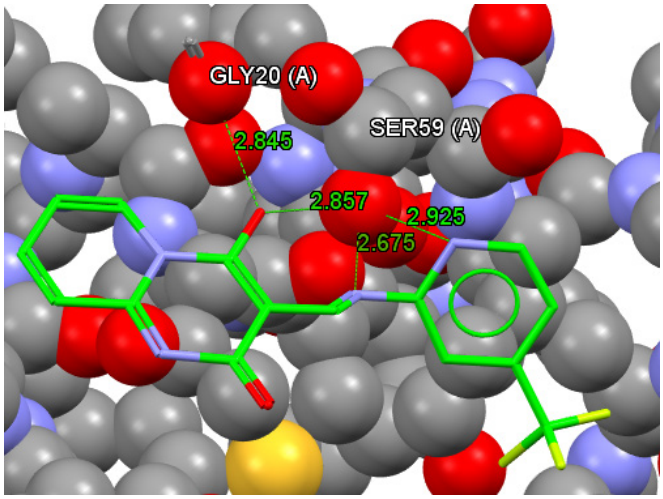

Figure 3: H-bond interaction for M3 binding with DHFR enzyme

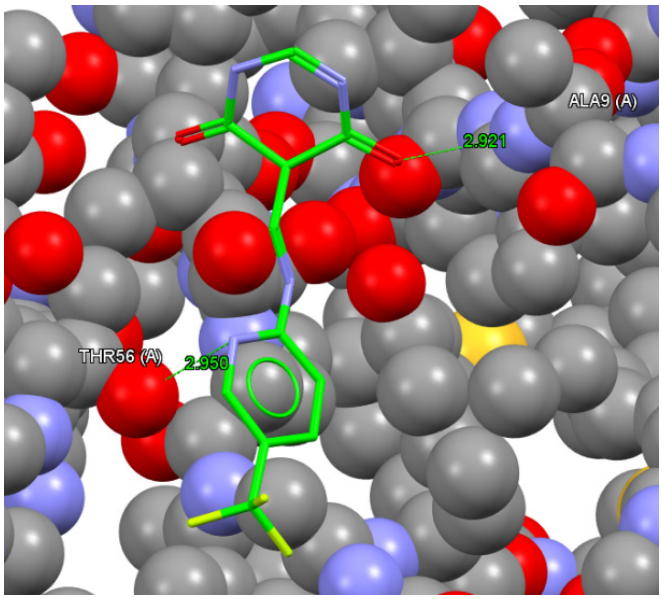

Figure 4: H-bond interaction for M4 binding with DHFR enzyme

with the anticancer assay. In addition, these compounds were predicted to have superior drug-likeness properties, as indicated by Insilico pharmacokinetic study. Finally, the synthesized compounds may be used as lead compounds in the design of new anticancer agents.

LIMITATIONS AND FUTURE STUDIES

The synthesized compounds were designed as non-classical Antifolate. So there is a need to assess their inhibitory activity against different folate pathway enzymes like DHFR and TS, also the need for other types of cancerous cell lines to a full assessment of antitumor activity.

ACKNOWLEDGMENT

The authors would like to express their gratitude for the laboratories and help provided by the faculty of pharmacy at Mustansiriyah University and the college of pharmacy at Uruk University.

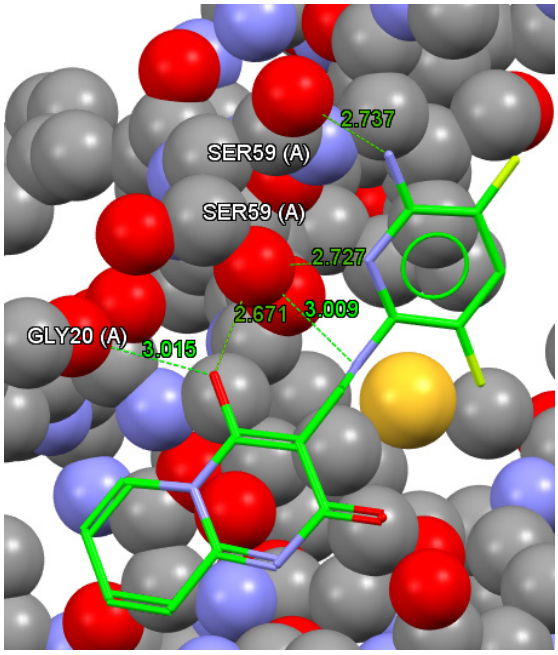

Figure 5: H-bond interaction for M5 binding with DHFR enzyme

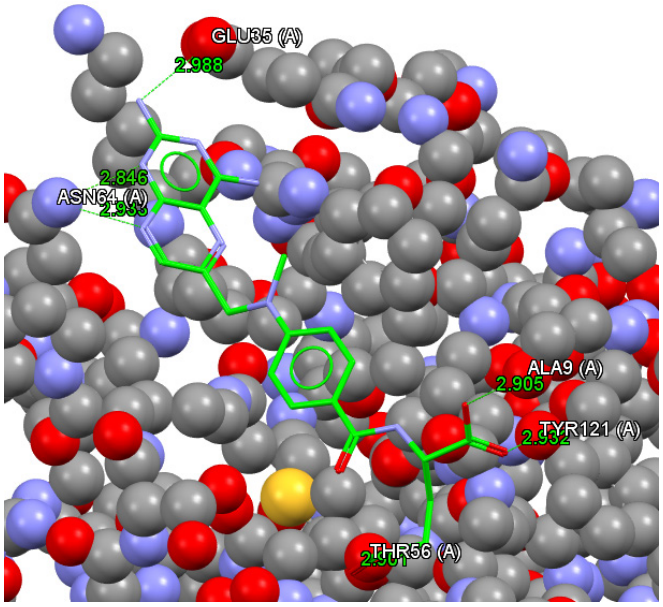

Figure 6: H-bond interaction for MTX binding with DHFR enzyme

REFERENCES

1. Nikolaou M, Pavlopoulou A, Georgakilas AG, Kyrodimos E. The challenge of drug resistance in cancer treatment: a current overview. Clinical & Experimental Metastasis. 2018;35(4):309-318.
2. Raimondi MV, Randazzo O, La Franca M, Barone G, Vignoni E, Rossi D, et al. DHFR inhibitors: reading the past for discovering novel anticancer agents. Molecules. 2019;24(6):1140.
3. Wohlgemuth R. Horizons of systems biocatalysis and renaissance of metabolite synthesis. Biotechnol. J. 2018;13(6):1700620.
4. Park SM, Yang H, Park SK, Kim HM, Kim BH. Design, synthesis, and anticancer activities of novel perfluoroalkyltriazole-appended 2′-deoxyuridines.Bioorganic Med. Chem. Lett. 2010;20(19):5831-5834.

5. Jameee N, Hosseini SS, Akrami HR, Dehghani Ashkzari M. Evaluation of cytotoxicity effect of Synthetic Pyridopyrimidine derivatives on the cancer vs. normal cell lines. Cell. Mol. Biol. J. 2019;10(37):35-52.
6. Kumar S, Deep A, Narasimhan B. A review on synthesis, anticancer and antiviral potentials of pyrimidine derivatives. Current Bioactive Compounds. 2019;15(3): 289-303.
7. Radwan MA, Alshubramy MA, Abdel-Motaal M, Hemdan BA, El-Kady DS. Synthesis, molecular docking and antimicrobial activity of new fused pyrimidine and pyridine derivatives. Bioorg. Chem. 2020;96:103516.
8. Kang D, Huo Z, Wu G, Xu J, Zhan P, Liu X. Novel fused pyrimidine and isoquinoline derivatives as potent HIV-1 NNRTIs: a patent evaluation of WO2016105532A1, WO2016105534A1 and WO2016105564A1. Expert Opin Ther Pat. 2017;27(4):383-391.
9. Abdel-Latif NA, Sabry NM, Mohamed AM, Abdulla MM. Synthesis, analgesic, and antiparkinsonian profiles of some pyridine, pyrazoline, and thiopyrimidine derivatives. Monatshefte für Chemie-Chemical Monthly. 2007;138(7):715-724.
10. Pamela S, Surendra V, Raj SU, Anirbandeep B, Giles D, Prakash T, Divakar G. Neurobehavioral assessments of Novel Pyrimidine derivative on experimental Zebra Fish. Journal of Innovation in Pharm. Sci. 2017;1(2):20-29.
11. Mohana Roopan S, Sompalle R. Synthetic chemistry of pyrimidines and fused pyrimidines: A review. Synthetic Communications. 2016;46(8):645-672.
12. Wang B, Zhao B, Chen Z-S, Pang L-P, Zhao Y-D, Guo Q, et al. Exploration of 1, 2, 3-triazole-pyrimidine hybrids as potent reversal agents against ABCB1-mediated multidrug resistance. Eur. J. Med. Chem 2018;143:1535-1542.
13. Gangjee A, Devraj R, McGuire JJ, Kisliuk RL. 5-arylthio substituted 2-amino-4-oxo-6-methylpyrrolo [2, 3-d] pyrimidine antifolates as thymidylate synthase inhibitors and antitumor agents. Journal of medicinal chemistry. 1995;38(22):4495-4502.
14. Vickers PJ, Townsend AJ, Cowan KH. Mechanisms of resistance to antineoplastic drugs. Developments in cancer chemotherapy: CRC Press; 2019;117-152.
15. Shirsat AJ, Bhagat SS, Rupnar BD, Dhas AK, Dixit P, Kakade GK. Synthesis, Characterization and Antimicrobial Activity Analysis of Some New Schiff Bases. J. Curr. Pharm. Res. 2019; 10(1):3528-3534.
16. Kumar RA, Sridevi K, Kumar NV, Nanduri S, Rajagopal S. Anticancer and immunostimulatory compounds from Andrographis paniculata. J. Ethnopharmacol 2004 Jun 1;92(2-3):291-295.
17. Snyder HR, Robison MM. Structure and Reactions of Malonyl-α-aminopyridine. I. J. Am Chem. Soc. 1952 Oct;74(19):4910-4916.
18. Eldredge CH, Mee JD, inventors; Eastman Kodak Co, assignee. Intermediates and the preparation and use thereof. United States patent US 1972;4(3):674-782.
19. Alwan S, Al-Kaabi J, Hashim R. Synthesis and preliminary antimicrobial activity of new Schiff bases of pyrido [1, 2-a] pyrimidine derivatives with certain amino acids. Med chem. 2014;4(9):635-639.
20. Hussain S, Cevik E, Tombuloglu H, Farag K, Said O. miRNA profiling in MCF-7 breast Cancer cells: seeking a new biomarker. J Biomedical Sci. 2019;8(2):3.
21. Barai AC, Paul K, Dey A, Manna S, Roy S, Bag BG, Mukhopadhyay C. Green synthesis of Nerium oleander-conjugated gold nanoparticles and study of its in vitro anticancer activity on MCF-7 cell lines and catalytic activity. Nano convergence. 2018;5(1): 1-9.
22. Okhti ZA, Al-Sudani BT, Abdalah ME. Study the Effect of Rubia Cordifolia Extract on Different Type of Cancer Cell Lines and Different Microbial. Systematic Reviews in Pharmacy. 2020;11(11):994-1000.
23. Kumar P, Nagarajan A, Uchil PD. Analysis of cell viability by the MTT assay. Cold spring harbor protocols. 2018 Jun 1;2018(6):pdb-rot095505.
24. Batiha GE, Beshbishy AM, Tayebwa DS, Adeyemi OS, Yokoyama N, Igarashi I. Evaluation of the inhibitory effect of ivermectin on the growth of Babesia and Theileria parasites in vitro and in vivo. Tropical medicine and health. 2019 Dec;47(1):1-2.
25. Ghanim ZS, Mahdi MF, Raauf AM. Molecular Docking, synthesis, anticancer assessment and ADME study of naproxen containing imidazole ring derivatives. Materials Today: Proceedings. 2021 Jun 5.
26. Van Bocxlaer K, Caridha D, Black C, Vesely B, Leed S, Sciotti RJ, Wijnant GJ, Yardley V, Braillard S, Mowbray CE, Ioset JR. Novel benzoxaborole, nitroimidazole and aminopyrazoles with activity against experimental cutaneous leishmaniasis. International J Parasitol-Drug and Drug Resistance. 2019;11:129-138.
27. Tripathi A, Misra K. Molecular docking: A structure-based drug designing approach. JSM Chem. 2017;5(2):1042-1047.
28. Cleves AE, Johnson SR, Jain AN. Electrostatic-field and surface-shape similarity for virtual screening and pose prediction. J. Comput. Aided Mol. Des. 2019;33(10):865-886.